PVT Studies on Dimer Liquid Crystals and Estimation of Transition Entropies at Constant Volume

Akihiro Abe* and Su Yong Nam

Department of Polymer Chemistry, Tokyo Institute of Technology, Ookayama, Meguro-ku, Tokyo 152, Japan

Received April 11, 1994; Revised Manuscript Received October 1, 1994[⊗]

ABSTRACT: Pressure−volume−temperature (*PVT*) measurements were performed on α,ω-bis[(4,4′-cyanobiphenylyl)oxy]alkane (CBA-*n*) dimer liquid crystals having $-O(CH_2)_nO-$ flexible spacers (n = 9, 10) between the 4,4′-cyanobiphenylyl ends. Both samples exhibit crystalline ↔ nematic (CN) and nematic ↔ isotropic (NI) transitions. The contribution in entropy ΔS_V caused by the volume change has been estimated by using the standard thermodynamic relation $\Delta S_V = -(\alpha/\beta)\Delta V_{tr}$, where ΔV_{tr} represents the transition volume, α the thermal expansion coefficient, and β the isothermal compressibility. The transition entropy $(\Delta S_{tr})_v$ at constant volume was elucidated by subtracting ΔS_v from the entropy change $(\Delta S_{tr})_p$ observed under constant pressure. By using the $(\Delta S_{ni})_p$ values derived from the Clapeyron equation, the constant-volume entropies $(\Delta S_{ni})_v$ at the NI transition were found to be 7.9 and 13.3 J mol^{-1} K^{-1}, respectively, for CBA-9 and -10. The values of $(\Delta S_{cn})_v$ for the CN transition were estimated on the basis of DSC data: 53.9 (CBA-9) and 62.4 J mol^{-1} K^{-1} (CBA-10). For both transitions, the correction for the volume change was found to be significant, ranging from 40 to 60% of the total transition entropy observed under constant pressure. Nevertheless, the odd−even character of the NI transition remains unaltered. As shown by comparison of $(\Delta S_{cn})_v$ and $(\Delta S_{ni})_v$, the major change (85%) takes place at the CN transition, the liberation of entropy at the NI interphase being much smaller (15%).

1. Introduction

In a series of papers,[1−5] we have studied the conformations of chain molecules variously involved in liquid crystals. Flexible chains, which tend to be a random coil in the isotropic state, are highly incompatible with liquid crystals. Phase equilibrium studies indicate that chain molecules such as *n*-alkanes, dimethyl ethylene glycol ethers, poly(ethylene glycol), or polystyrene are very disruptive to the nematic order and thus are allowed to exist only in a limited amount in liquid crystals.[6−8] Flexible tails appended to a mesogenic core unit are, on the contrary, known to play an important role in stabilizing the anisotropic phase of the low-molar-mass (monomer) liquid crystals (MLC). The nematic−isotropic transition temperature and the associated thermodynamic quantities sometimes exhibit a weak odd−even oscillation when plotted against the number of constituent atoms of the tail.[9] The NMR/RIS analysis indicates that the conformational distribution of the tail tends to be somewhat restricted in the nematic environment as compared with the distribution permitted in the isotropic state.[3]

A more pronounced odd−even effect has been observed in the main chain type dimer (DLC) and polymer liquid crystals (PLC) comprising rigid mesogenic cores joined through a flexible spacer.[4,10,11] The simplest example of such spacers may be of the type $-O(CH_2)_nO-$. In these systems, the orientational order parameter of the mesogenic core axis oscillates with the number of methylene units n, suggesting that the order−disorder transition of the mesogenic core is coupled with the conformational change of the flexible spacer.[5,12] In this respect, DLCs as well as PLCs are very different from simple monomer liquid crystals. The conformation of such spacers has been elucidated for several examples of nematic liquid crystals from the relevant ^{2}H NMR data.[4,13−15] Although the results reported from various laboratories seem to vary somewhat depending on the models adopted in the simulation of the spectra, all suggest that flexible spacers prefer to take extended conformations in the nematic state. In an ideal crystalline state, molecules are aligned in perfect order, only the most preferred conformation being permitted for the spacer. The structural characteristics of chain molecules in the crystalline, liquid crystalline, and isotropic liquid states must manifest themselves in the configurational entropy of the system upon phase transitions. The phase transition of a mesogenic compound is usually described by the competition between the anisotropic dispersion energy and the orientational entropy. Attempts to include the steric contribution explicitly in the thermodynamic expression often lead to an appreciable overestimate of the order parameter at the transition.[16] In this respect, the role of the steric interaction is somewhat obscure. For the main chain LCs, the contribution arising from the conformational change of the flexible spacer should also become important.

In fact, it is well-known for various semiflexible polymers that the entropy of fusion is of prime importance in establishing the melting temperature.[17,18] The rotational isomeric character of chain molecules provides a useful method to estimate the partition function of the chain configuration in the fluid state. The configurational entropy change at the phase transition may be derived as the difference between the two relevant states. For a variety of conventional polymers, the entropy change calculated in this manner is usually in good agreement with the experimental estimate of the entropy of melting at constant volume. Although the physical basis of such an entropy separation is somewhat controversial,[19] the technique is well accepted for long chain molecules. A similar treatment may thus be applicable to the liquid crystalline system under consideration.

In this work, we have performed pressure−volume−temperature (*PVT*) measurements on α,ω-bis[(4,4′-cyanobiphenylyl)oxy]alkane (CBA-*n*) DLC samples

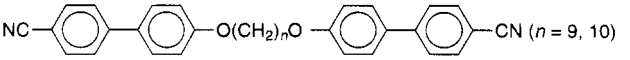

⊗ Abstract published in *Advance ACS Abstracts*, December 1, 1994.

0024-9297/95/2228-0090$09.00/0

The contribution in entropy caused by the volume change at a phase transition can be expressed as[17]

$$\Delta S_v = \gamma \Delta V_{tr} = -(\alpha/\beta)\Delta V_{tr} \quad (1)$$

where

$$\alpha = (\partial \ln v/\partial t)_p$$

$$\beta = -(\partial \ln v/\partial p)_t \quad (2)$$

$$\gamma = (\partial p/\partial t)_v$$

ΔV_{tr} is the volume change, γ is the thermal pressure coefficient at the transition, α is the thermal expansion coefficient at constant pressure, and β is the isothermal compressibility at constant temperature. Hereafter subscript tr represents a transition at the crystal–nematic (CN) or nematic–isotropic (NI) interphase. The entropy change at constant volume $(\Delta S_{tr})_v$ is related to that at constant pressure $(\Delta S_{tr})_p$ by

$$(\Delta S_{tr})_v = (\Delta S_{tr})_p - \Delta S_v \quad (3)$$

Dimer liquid crystals CBA-9 and -10 exhibit two well-defined phase transitions as a function of temperature: crystal ↔ nematic liquid crystal ↔ isotropic melt. The transition entropies $(\Delta S_{cn})_v$ and $(\Delta S_{ni})_v$, respectively defined at the CN and NI interphase, can be estimated by using eq 3. For the latter transition, a distinct odd–even effect has been observed in various thermodynamic quantities as a function of the number of atoms involved in the spacer. It should be interesting to know if a similar empirical rule still holds for the entropy change under constant volume. For this reason, we have chosen two CBA samples with $n = 9$ and 10.

2. Experimental Section

The preparation of CBA-9 and -10 has been described elsewhere.[10] These samples exhibit an enantiotropic nematic mesophase by polarizing microscopic examination:

CBA-9: C 133 °C N 173 °C I

CBA-10: C 165 °C N 185 °C I

Thermal transitions were measured with a Perkin-Elmer differential scanning calorimeter (DSC) calibrated with indium. Samples (approximately 0.6 mg) were loaded into aluminum pans. Heating rates of 10 deg min^{-1} were employed in most of the DSC scans. In order to provide the same thermal history, each sample was heated to 210 °C and subsequently cooled to room temperature. The data were collected from the second-scan heating curves. Temperatures corresponding to the onset of phase transformation were recorded for each endotherm or exotherm.

A *PVT* apparatus manufactured by GNOMIX Co. (Boulder, CO) was used to determine the change in specific volume as a function of temperature and pressure. The apparatus consists of a bellows cell containing about 1–2 g of sample and mercury as a confining fluid. The deflection of the bellows under temperature and pressure changes is measured by a transformer. The volume change of the sample can be calculated by making allowance for the known *PVT* properties of mercury. In the isothermal mode, volume readings were recorded over a pressure range from 10 to 100 MPa at a fixed interval (10 MPa) while the temperature was kept invariant. The temperature was then changed by 10 °C and the process repeated. The measurements were also performed in the isobaric mode (at 10 and 40 MPa) by ramping the temperature (30–250 °C) up or down. The absolute accuracy of the device has been claimed as $(3–4) \times 10^{-3}$ cm^3 g^{-1}, but volume changes much smaller than this figure can be resolved. Prior to the *PVT* measurements, the densities of the sample were determined with a pycnometer (volume ca. 50 mL) at 30 °C under atmospheric pressure. About 2–3 g of sample was charged and calibration was carried out by using reagent grade ethanol. Density: CBA-9, 1.139 g/cm^3; CBA-10, 1.135 g/cm^3.

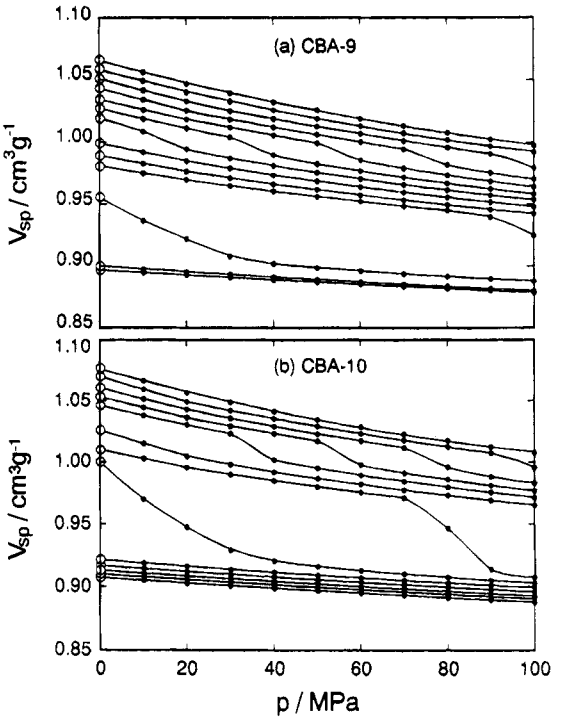

Figure 1. Volume–pressure isotherms for (a) CBA-9 and (b) CBA-10 from 120 to 240 °C by 10 °C intervals. Open circles indicate specific volumes at $p = 0$ estimated by extrapolation.

3. Results

Some representative *PVT* data collected in the isothermal mode are indicated in Figures 1 ($V–P$ plot) and 2 ($V–T$ plot). The measurements were performed first by raising temperature at a 10 deg interval up to 250 °C and then continued in a similar manner during the cooling process. The specific volumes at zero pressure ($p = 0$) were estimated from those observed at higher pressures: extrapolations were executed by using polynomial expressions. The extrapolated values are indicated by open circles in these diagrams. Figure 1 clearly shows that the phase transition temperatures (T_m and T_{ni}) exhibit an appreciable pressure dependence in both CBA samples. The compressibilities β in the low-pressure region are one of the major interests in this work. The values estimated in the nematic and isotropic phases slightly above the transition temperatures are listed in Table 1, where T_m, T_c, and T_{ni} were taken to be the midpoint of the corresponding transitions indicated in the $V–T$ diagram (cf. Figure 2). Since the nematic phase is stable over a limited temperature range in both samples, the uncertainty involved in the extrapolation is comparatively large as indicated in Table 1.

In Figure 3, the $V–T$ relations estimated at zero pressure ($p = 0$) are compared with those directly determined by an isobaric (heating) process at higher pressures (10 and 40 MPa). The results obtained by the two independent measurements are moderately consistent. It is known for typical liquid crystals that the thermal expansion coefficient increases rapidly in the

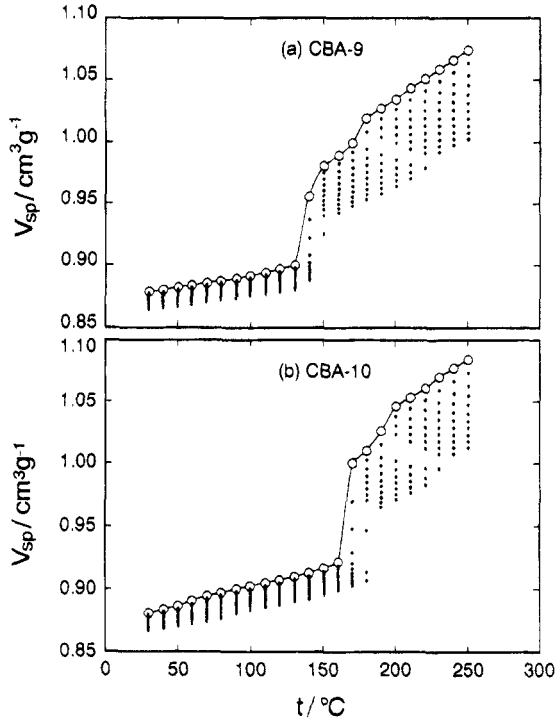

Figure 2. Volume vs temperature relations for (a) CBA-9 and (b) CBA-10 from 10 to 100 MPa for each 10 MPa. Extrapolated values to zero pressure are indicated by open circles. For simplicity, v_{sp}–t curves are drawn only for $p = 0$. (For experimental details, see Section 2.)

Table 1. Experimental Values of $\beta = -(\partial \ln v_{sp}/\partial p)_t$ Estimated in the Low-Pressure Region for the Nematic and Isotropic States Slightly above the Transition Temperature

	nematic, in the vicinity of T_m or T_c		isotropic, in the vicinity of T_{ni}	
thermal process	T_m or T_c (°C)	$\beta \times 10^3$ (MPa^{-1})	T_{ni} (°C)	$\beta \times 10^3$ (MPa^{-1})
		CBA-9		
heating	139	1.24 ± 0.10	174	2.26 ± 0.01
cooling	125	1.34 ± 0.11	174	2.60 ± 0.01
		CBA-10		
heating	165	1.59 ± 0.20	190	2.36 ± 0.01
cooling	164	1.87 ± 0.08	189	2.57 ± 0.01

pretransition region as the temperature approaches T_{ni} and it decreases with increasing temperature above T_{ni}.[21] These characteristics may be confirmed for both CBA samples in the V–T plots derived from the isobaric measurements at 10 and 40 MPa (see Figure 3). Since the V–T relation at $p = 0$ involves extrapolation from higher pressures, a detailed investigation of the critical divergence phenomenon[16] is improbable. Examples of the V–T relation obtained during a heating–cooling cycle at 10 MPa are included in the insets of Figure 3. In both samples, melting (T_m on heating) was observed at a higher temperature than crystallization (T_c on cooling). In contrast, the transition at the NI phase boundary remains almost unaffected by the experimental conditions.

The specific volume–temperature (v_{sp}–t) plots for $p = 0$ were fitted to a polynomial function by the least-squares method. Expressions for the thermal expansion coefficient α were also obtained in a polynomial form from the ln v_{sp} vs t curves. Within the experimental accuracy, the results were found to be most satisfactorily represented by linear relations such as

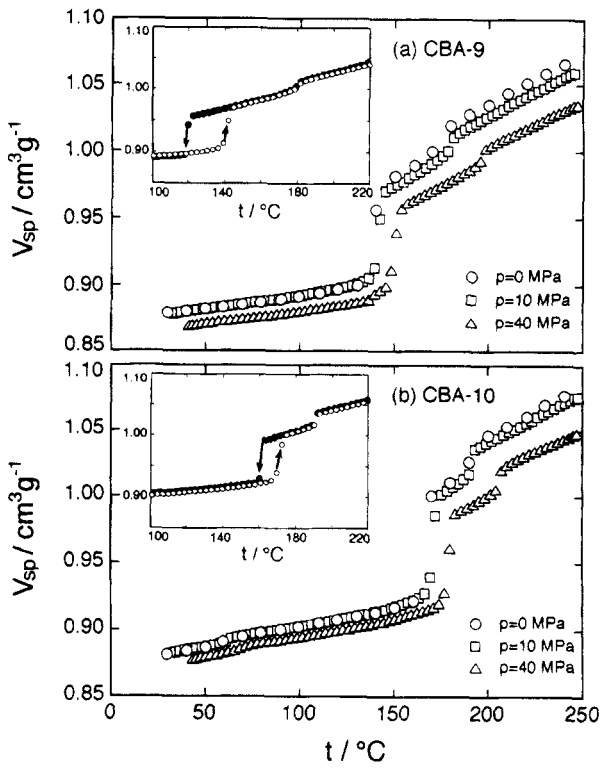

Figure 3. Comparison of v_{sp}–t relations derived from the measurements in the isothermal ($p = 0$) and isobaric modes ($p = 10$ and 40 MPa): (a) CBA-9 and (b) CBA-10. Open circles for $p = 0$ were taken from Figure 2. Shown in the inset are the v_{sp}–t curves obtained under an isobaric condition ($p = 10$ MPa) with ascending and descending temperatures, indicated respectively by white and black dots.

$$v_{sp}(t) = v(t_0) + a(t - t_0) \tag{4}$$

and

$$\alpha(t) = \alpha(t_0) + b(t - t_0) \tag{5}$$

The coefficients of these expressions are summarized in Table 2. The volume changes ΔV_{tr} at T_m, T_c, and T_{ni} can be obtained from these v_{sp}–t relations. The values of ΔV_{tr} thus determined correspond to the difference between the two stable states. Variations of ΔV_{tr} with pressure observed during the heating and cooling process are illustrated in Figure 4, for CBA-9 and -10. While the volume change ΔV_{cn} at the CN transition tends to be moderately depressed as pressure increases, the corresponding transition volume ΔV_{ni} at the NI interphase remains nearly invariant for both samples. For given transitions, a pair of ΔV_{tr} values observed on the heating and cooling process are reasonably consistent except for the CN transition of CBA-9, for which a relatively larger supercooling was observed at the crystallization: $T_m - T_c = 14$ °C. Correspondingly, the values of ΔV_{cn} obtained at T_c are lower by about 20% than those at T_m for this sample. The transition volumes ΔV_{tr} estimated for $p = 0$ are listed in Table 3, where the thermal expansion coefficients α obtained for the nematic and isotropic phases in the vicinity of transition temperatures are also accommodated.

The enthalpy changes under atmospheric pressure can be customarily measured by using DSC. The transition temperatures T_{cn} and T_{ni} and the heats ΔH_{tr} determined by DSC are given in Table 4. The transition temperatures shown in the table are lower than those estimated previously from the v_{sp}–t curve (cf. Tables 1

Table 2. Specific Volumes v_{sp} and Thermal Expansion Coefficients $\alpha = (\partial \ln v_{sp}/\partial t)_p$ Estimated for $p = 0$[a]

CBA-9

heating	cooling
crystalline phase	
range of temperatures: 30–139 °C	range of temperatures: 40–125 °C
$v_{sp}(t) = 0.8785 + 1.8738 \times 10^{-4}(t - 30)$	$v_{sp}(t) = 0.8833 + 2.8806 \times 10^{-4}(t - 40)$
$\alpha(t) = 4.2490 \times 10^{-4} + 5.3041 \times 10^{-7}(t - 30)$	$\alpha(t) = 6.6212 \times 10^{-4} + 4.5825 \times 10^{-7}(t - 40)$
nematic phase	
range of temperatures: 139–174 °C	range of temperatures: 125–174 °C
$v_{sp}(t) = 0.9717 + 8.1718 \times 10^{-4}(t - 139)$	$v_{sp}(t) = 0.9674 + 7.4263 \times 10^{-4}(t - 125)$
$\alpha(t) = 21.8446 \times 10^{-4} + 2.4846 \times 10^{-7}(t - 139)$	$\alpha(t) = 19.6550 \times 10^{-4} + 2.7685 \times 10^{-7}(t - 125)$
isotropic phase	
range of temperatures: 174–250 °C	range of temperatures: 174–250 °C
$v_{sp}(t) = 1.0148 + 7.8017 \times 10^{-4}(t - 174)$	$v_{sp}(t) = 1.0196 + 8.3975 \times 10^{-4}(t - 174)$
$\alpha(t) = 21.0019 \times 10^{-4} + 36.9276 \times 10^{-7}(t - 174)$	$\alpha(t) = 23.7890 \times 10^{-4} + 8.4809 \times 10^{-7}(t - 174)$

CBA-10

heating	cooling
crystalline phase	
range of temperatures: 30–165 °C	range of temperatures: 130–164 °C
$v_{sp}(t) = 0.8818 + 2.902 \times 10^{-4}(t - 30)$	$v_{sp}(t) = 0.9075 + 4.1695 \times 10^{-4}(t - 130)$
$\alpha(t) = 7.8955 \times 10^{-4} - 11.4676 \times 10^{-7}(t - 30)$	$\alpha(t) = 10.2467 \times 10^{-4} + 8.1052 \times 10^{-7}(t - 130)$
nematic phase	
range of temperatures: 165–190 °C	range of temperatures: 164–189 °C
$v_{sp}(t) = 0.9952 + 10.0 \times 10^{-4}(t - 165)$	$v_{sp}(t) = 0.9933 + 8.8822 \times 10^{-4}(t - 164)$
$\alpha(t) = 27.2667 \times 10^{-4} + 4.5159 \times 10^{-7}(t - 165)$	$\alpha(t) = 24.2667 \times 10^{-4} + 1.0099 \times 10^{-7}(t - 164)$
isotropic phase	
range of temperatures: 190–250 °C	range of temperatures: 189–250 °C
$v_{sp}(t) = 1.0380 + 7.7108 \times 10^{-4}(t - 190)$	$v_{sp}(t) = 1.0352 + 7.973 \times 10^{-4}(t - 189)$
$\alpha(t) = 22.1709 \times 10^{-4} + 6.8987 \times 10^{-7}(t - 190)$	$\alpha(t) = 23.9039 \times 10^{-4} - 17.9465 \times 10^{-7}(t - 189)$

[a] The mathematical expressions are defined in eqs 4 and 5: $v_{sp}/(cm^3\ g^{-1})$, α/deg^{-1}, $t/°C$.

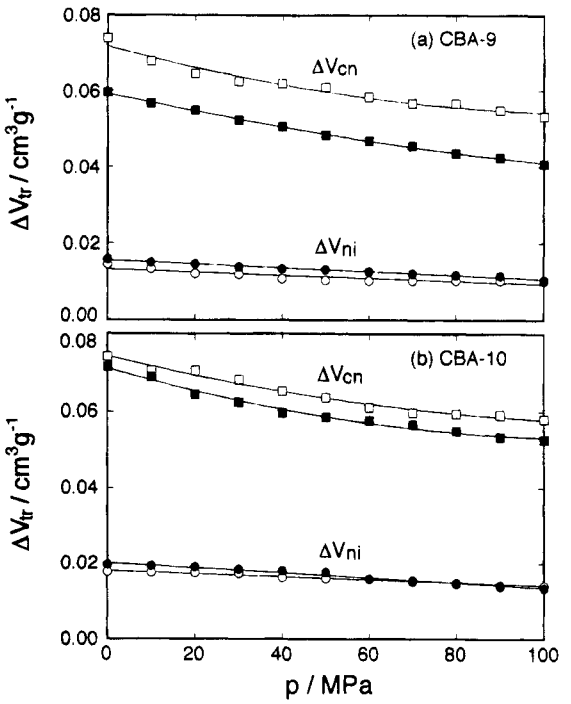

Figure 4. Variation of transition volumes ΔV_{cn} (squares) and ΔV_{ni} (circles) as a function of pressure. The data points collected from the heating and cooling processes are distinguished respectively by open and filled symbols.

and 3). Except for the crystallization temperature (T_c), differences between the DSC and *PVT* data are marginal. The depressions $\Delta T = T_m - T_c$ amount to 30–40 °C in DSC while they are only 14 and 1 °C, respectively, for CBA-9 and -10 in *PVT*. The degree of supercooling on crystallization tends to be enhanced when the cooling rate of the sample is higher. The

Table 3. Experimental Values of ΔV_{tr} and $\alpha = (\partial \ln v_{sp}/\partial t)_p$ Estimated for $p = 0$ in the Nematic and Isotropic Regions

	nematic, in the vicinity of T_m or T_c			isotropic, in the vicinity of T_{ni}		
thermal process	T_m or T_c (°C)	ΔV_{cn} ($cm^3\ g^{-1}$)	$\alpha \times 10^3$ (K^{-1})	T_{ni} (°C)	ΔV_{ni} ($cm^3\ g^{-1}$)	$\alpha \times 10^3$ (K^{-1})
			CBA-9			
heating	139	0.0730	2.184	174	0.0145	2.100
cooling	125	0.0594	1.966	174	0.0159	2.379
			CBA-10			
heating	165	0.0745	2.727	190	0.0178	2.217
cooling	164	0.0716	2.427	189	0.0197	2.390

Table 4. Summary of DSC Data

	CN transition			NI transition		
thermal process	T_m or T_c (°C)	ΔH_{cn} (kJ mol^{-1})	ΔS_{cn} (J mol^{-1} K^{-1})	T_{ni} (°C)	ΔH_{ni} (kJ mol^{-1})	ΔS_{ni} (J mol^{-1} K^{-1})
			CBA-9			
heating	134.8	48.93	119.9	173.0	4.16	9.3
cooling	104.0	50.50	133.9	171.5	4.52	10.2
			CBA-10			
heating	164.6	56.84	129.8	184.0	9.42	20.6
cooling	124.8	54.61	137.2	183.0	10.47	23.0

values of ΔH_{tr} and the corresponding ΔS_{tr} were estimated by measuring the area of the DSC peaks in the usual manner. The observed values fluctuate within ±10–15% around those listed in Table 4.

The enthalpy changes may be alternatively estimated with the aid of the Clapeyron equation:

$$\Delta H_{tr} = T_{tr} \Delta V_{tr}\, dp/dt \qquad (6)$$

where dp/dt designates the slope of the phase boundary

Table 5. Values of ΔH_{ni} and ΔS_{ni} Estimated on the Basis of the Clapeyron Equation

sample	thermal process	T_{ni} (°C)	ΔV_{ni} (cm^3 mol^{-1})	dp/dt (MPa K^{-1})	ΔH_{ni} (kJ mol^{-1})	ΔS_{ni} (J mol^{-1} K^{-1})
CBA-9	heating	174	7.45	2.00	6.66	14.9
	cooling	174	8.17	2.05	7.49	16.7
CBA-10	heating	190	9.39	2.35	10.22	22.1
	cooling	189	10.38	2.36	11.32	24.5

curve in the low-pressure region. For the NI transition, the values of dp/dt estimated from the measurements in the isothermal (Figure 2) and isobaric modes (Figure 3) were mutually consistent. The enthalpy ΔH_{ni} and entropy changes ΔS_{ni} calculated according to eq 6 are listed in Table 5. The difference between the *PVT* (Table 5) and DSC methods (Table 4) amounts to 10–30%. While the heats determined on the basis of *PVT* data are a measure of the discontinuity of a first-order transition at a given temperature T_{tr}, those from calorimetric measurements may include some additional contribution due to pretransition phenomena occurring on both sides of the transition. In addition, some difficulty is inevitably invoked in selecting a baseline in the DSC method. In the following treatment, the values of ΔS_{ni} obtained by the *PVT* method and tabulated in Table 5 will be adopted for the estimation of entropy changes at constant volume $(\Delta S_{ni})_v$. As revealed in Figures 2 and 3, the crystalline–nematic phase boundary curves are less sensitive to pressure, and the values of dp/dt estimated from these two figures inevitably include large uncertainties. The use of eq 6 thus failed to give any reasonable assessment of enthalpies for the CN transition. The enthalpy changes ΔH_{cn} are therefore not included in Table 5. In the following treatment, the values of $(\Delta S_{cn})_p$ for the CN transition were borrowed from the DSC measurements.

In Table 6, ΔV_{tr}, γ, ΔS_v (cf. eq 1), and the transition entropies at constant volume $(\Delta S_{tr})_v$, defined as the difference between $(\Delta S_{tr})_p$ and ΔS_v in eq 3, are listed. In these calculations, the values of $(\Delta S_{tr})_p$ were taken from Table 4 for the CN transition and from Table 5 for the NI transition. As shown in Table 4, the difference ΔT between the crystallization temperature T_c and the melting temperature T_m is sizable, especially in the DSC measurements, suggesting that supercooling takes place during crystallization. The enthalpy changes ΔH_{cn} observed during cooling may include some effect arising from this source. The values of $(\Delta S_{cn})_v$ associated with the cooling process are somewhat larger than the corresponding results estimated on the basis of the heating data. For the NI transition, the supercooling phenomenon is less marked, and thus the agreement between the heating and cooling processes is reasonable for various thermodynamic quantities including $(\Delta S_{ni})_v$. Although the precise estimation of errors involved in the elucidation of entropies is difficult, the uncertainties in the final results could amount to 30–40% of $(\Delta S_{ni})_v$.

4. Discussion

For the reason stated above, the experimental data collected during the heating process may be better suited for the thermodynamic analysis under consideration. Since this is the first *PVT* report on DLCs, the results obtained from the cooling process are also included. As shown in Table 3, the volume changes ΔV_{ni} observed at the NI transition are about 20–30% relative to the corresponding discontinuity ΔV_{cn} at the CN interphase. The observed values of ΔV_{ni} = ca. 2×10^{-2} cm^3 g^{-1} are substantially larger than those reported for conventional MLCs[21] but smaller than those reported for semicrystalline main chain type PLCs.[22] The other thermodynamic properties of the nematic phase such as the thermal expansion coefficient α and compressibility β also exceed those found for simple MLCs.[21,23] The thermal pressure coefficients γ estimated at T_{ni} are 0.93 and 0.94 MPa K^{-1} (on heating), respectively, for CBA-9 and -10. These values are somewhat smaller than those reported for 5CB and 7CB.[21] In this work, the pressure–temperature coefficients γ were obtained as the ratio $-\alpha/\beta$. The reliability of γ values may be improved by directly determining the isochore in the low-pressure region. Studies along this line are in progress.

The values of $(\Delta S_{ni})_v$ found in this work (8–15 J mol^{-1} K^{-1}) are appreciably larger than those estimated for relevant MLCs such as 4′-*n*-alkyl-4-cyanobiphenyls or 4′-*n*-alkoxy-4-cyanobiphenyls, for which Orwoll et al. reported entropy changes in the range 0.2–0.8 J mol^{-1} K^{-1}.[21] The results indicate that the constant-volume transition entropy could be enhanced dramatically by incorporation of a flexible spacer.

For both CN and NI transitions, the correction term ΔS_v for the volume expansion was found to be significant, ranging from 40 to 60% of the total transition entropy observed under constant pressure. However, the odd–even character of the NI transition was unaltered by introducing the correction due to the volume change. As shown by comparison of $(\Delta S_{cn})_v$ and $(\Delta S_{ni})_v$, the major change (80–90%) takes place at the C → N transition, the liberation of entropy at the N → I interphase being much smaller (10–20%). The sum of $(\Delta S_{cn})_v$ and $(\Delta S_{ni})_v$ should approximately represent the constant-volume entropy change on going from the crystalline state to the isotropic melt. From Table 6, we obtain 61.8 and 75.7 J mol^{-1} K^{-1}, respectively, for CBA-9 and -10. These values are nearly equivalent to those (80–90 J mol^{-1} K^{-1}) estimated for a $-(CH_2)_m-$ sequence (m = 9–10) buried in the polymethylene chain. The results suggest that the conformational contribution

Table 6. Estimation of the Entropy Change at Constant Volume for CBA-*n* with *n* = 9 and 10[a]

	CN transition				NI transition			
thermal process	ΔV_{cn} (cm^3 mol^{-1})	γ (MPa K^{-1})	ΔS_v (J mol^{-1} K^{-1})	$(\Delta S_{cn})_v$[b] (J mol^{-1} K^{-1})	ΔV_{ni} (cm^3 mol^{-1})	γ (MPa K^{-1})	ΔS_v (J mol^{-1} K^{-1})	$(\Delta S_{ni})_v$[c] (J mol^{-1} K^{-1})
				CBA-9				
heating	37.5	1.76	66.0	53.9	7.5	0.93	7.0	7.9
cooling	30.5	1.47	44.7	89.2	8.2	0.92	7.5	9.2
				CBA-10				
heating	39.3	1.72	67.4	62.4	9.4	0.94	8.8	13.3
cooling	37.8	1.30	49.1	88.1	10.4	0.93	9.7	14.8

[a] Estimated according to eq 3. [b] Values of $(\Delta S_{cn})_p$ required in this estimation were taken from Table 4. [c] Values of $(\Delta S_{ni})_p$ were obtained from Table 5.

is an important factor involved in the phase transition of main chain type LCs.

Finally, we wish to emphasize that the *PVT* data reported above may be useful to investigate the molecular aspect of CN and NI transitions. As indicated by the X-ray examination, the dimer samples are highly crystalline in the solid state.[24] The RIS analysis of ^2H NMR quadrupolar splitting data should provide information regarding the spacer conformation in the nematic state.[1-5] The spatial configurations of these molecules in the isotropic state may be approximated by those elucidated from solution properties such as the anisotropy of polarizability and the dipole moment.[25] The magnitude of the conformational-entropy change can be evaluated on the basis of the conformational distributions of the spacer obtained in the liquid crystalline and isotropic-liquid states. Comparison of the results with the transition entropies at constant volume determined in this work should reveal the relative importance of the flexible part in establishing the individual phase transitions. This is the subject of the following paper.[26]

Acknowledgment. The authors are grateful to the Asahi Glass Foundation for financial support of this work. We wish to thank Mr. T. Horiguchi, Mr. T. Matsuzaki, and Mr. S. Matsui of Matsushita Inter-Techno Co., Ltd., for their assistance in *PVT* measurements.

References and Notes

(1) Abe, A. *Macromolecules* **1984**, *17*, 2280. Abe, A. *Makromol. Chem., Macromol. Symp.* **1992**, *53*, 13.
(2) Sasanuma, Y.; Abe, A. *Polym. J.* **1991**, *23*, 117. Abe, A.; Iizumi, E.; Sasanuma, Y. *Polym. J.* **1993**, *25*, 1087. Abe, A.; Iizumi, E.; Kimura, N. *Liq. Cryst.* **1994**, *16*, 655.
(3) Abe, A.; Furuya, H. *Mol. Cryst. Liq. Cryst.* **1988**, *159*, 99. Abe, A.; Kimura, N.; Nakamura, M. *Makromol. Chem. Theory Simul.* **1992**, *1*, 401.
(4) Abe, A.; Furuya, H. *Macromolecules* **1989**, *22*, 2982. Abe, A.; Shimizu, R. N.; Furuya, H. *Ordering in Macromolecular Systems*; Teramoto, A., Kobayashi, M., Norisuye, T., Eds.; Springer-Verlag: Berlin, Heidelberg, 1994; p 139.
(5) Furuya, H.; Dries, T.; Fuhrmann, K.; Abe, A.; Ballauff, M.; Fischer, E. W. *Macromolecules* **1990**, *23*, 4122. Furuya, H.; Abe, A.; Fuhrmann, K.; Ballauff, M.; Fischer, E. W. *Macromolecules* **1991**, *24*, 2999.
(6) Martire, D. E. *The Molecular Physics of Liquid Crystals*; Luchhurst, G. R., Gray, G. W., Eds.; Academic Press: New York, 1979; Chapters 10, 11. Oweimreen, G. A.; Lin, G. C.; Martire, D. E. *J. Phys. Chem.* **1979**, *83*, 2111. Oweimreen, G. A.; Martire, D. E. *J. Chem. Phys.* **1980**, *72*, 2500.
(7) Kronberg, B.; Gilson, D. F. R.; Patterson, D. *J. Chem. Soc., Faraday Trans. 2* **1976**, *72*, 1673, 1686.
(8) Orendi, H.; Ballauff, M. *Liq. Cryst.* **1989**, *6*, 497; *Ber. Bunsenges. Phys. Chem.* **1992**, 96.
(9) Kelker, H.; Hatz, R. *Handbook of Liquid Crystals*; Verlag Chemie: Weinheim, 1980.
(10) Emsley, J. W.; Luckhurst, G. R.; Shilstone, G. N. *Mol. Cryst. Liq. Cryst.* **1984**, *102*, 223.
(11) Blumstein, A.; Thomas, O. *Macromolecules* **1982**, *15*, 1264.
(12) Toriumi, H.; Furuya, H.; Abe, A. *Polym. J.* **1985**, *17*, 895.
(13) Yoon, D. Y.; Brückner, S. *Macromolecules* **1985**, *18*, 651. Yoon, D. Y.; Brückner, S.; Volksen, W.; Scott, J. C.; Griffin, A. C. *Faraday Discuss. Chem. Soc.* **1985**, *79*, 41. Brückner, S.; Scott, J. C.; Yoon, D. Y.; Griffin, A. C. *Macromolecules* **1985**, *18*, 2709.
(14) Samulski, E. T.; Gauthier, M. M.; Blumstein, R. B.; Blumstein, A. *Macromolecules* **1984**, *17*, 479. Griffin, A. C.; Samulski, E. T. *J. Am. Chem. Soc.* **1985**, *107*, 2975; *Faraday Discuss. Chem. Soc.* **1985**, *79*, 7. Photinos, D. J.; Poon, C. D.; Samulski, E. T.; Toriumi, H. *J. Phys. Chem.* **1992**, *96*, 8176. Photinos, D. J.; Samulski, E. T.; Toriumi, H. *J. Chem. Soc., Faraday Trans.* **1992**, *88*, 1875.
(15) Emsley, J. W.; Heaton, N. J.; Luckhurst, G. R.; Shilstone, G. N. *Mol. Phys.* **1988**, *64*, 377. Cheung, S. T. W.; Emsley, J. W. *Liq. Cryst.* **1993**, *13*, 265.
(16) Vertogen, G.; de Jeu, W. H. *Thermotropic Liquid Crystals, Fundamentals*; Springer-Verlag: Berlin, 1988.
(17) Mandelkern, L. *Crystallization of Polymers*; McGraw-Hill: New York, 1964.
(18) Abe, A. *Macromolecules* **1980**, *13*, 546.
(19) Wunderlich, B.; Czornyj, G. *Macromolecules* **1977**, *10*, 906. Bleha, T. *Polymer* **1985**, *26*, 1638.
(20) Zoller, P.; Bolli, P.; Pahud, V.; Ackermann, H. *Rev. Sci. Instrum.* **1976**, *47*, 948.
(21) Stimpfle, R. M.; Orwoll, R. A.; Schott, M. E. *J. Phys. Chem.* **1979**, *83*, 613. Orwoll, R. A.; Sullivan, V. J.; Campbell, G. C. *Mol. Cryst. Liq. Cryst.* **1987**, *149*, 121.
(22) Walsh, D. J.; Dee, G. T.; Wojtkowski, P. W. *Polymer* **1989**, *30*, 1467. GNOMIX PVT Apparatus Catalogue, 1991, pp 21, 22.
(23) Kuss, E. *Mol. Cryst. Liq. Cryst.* **1978**, *47*, 71.
(24) Malpezzi, L.; Brückner, S.; Galbiati, E.; Luckhurst, G. R. *Mol. Cryst. Liq. Cryst.* **1991**, *195*, 179.
(25) Furuya, H.; Okamoto, S.; Abe, A.; Petekidis, G.; Fytas, G., to be published.
(26) Abe, A.; Furuya, H.; Shimizu, R. N.; Nam, S. Y. *Macromolecules* **1995**, *28*, 96.

MA941040O